

Aerodynamic Characteristics of a Delta Wing at High Angles of Attack

Akira Oyama¹

JAXA Institute of Space and Astronautical Science, Sagamihara, Kanagawa, 229-8510, Japan

Genta Imai²

University of Tokyo, Bunkyo, Tokyo, 113-8656, Japan

Akira Ogawa³

Tokyo Denki University, Hatoyama, Saitama, 350-0394, Japan

and

Kozo Fujii⁴

JAXA Institute of Space and Astronautical Science, Sagamihara, Kanagawa, 229-8510, Japan

Nomenclature

b	=	half span length
c	=	wing root chord length
C_N	=	normal force coefficient
C_{MP}	=	pitching moment coefficient about the apex of the wing
C_{MR}	=	rolling moment coefficient about the wing root
C_p	=	local pressure coefficient
F_N	=	normal force acting on the upper and lower surfaces
M_P	=	pitching moment about the apex of the wing
M_R	=	rolling moment about the wing root
M_N	=	the component of Mach number normal to the leading edge
M_∞	=	free-stream Mach number
Re	=	Reynolds number
x	=	chordwise position from the apex of the wing
y	=	spanwise position from the wing root
α	=	angles of attack (deg)
α_N	=	the component of angle of attack normal to the leading edge (deg)

I. Introduction

Many supersonic aircrafts use delta wing and they often fly at high angles of attack. For example, in landing or taking off phase, they need to fly at very high angle of attack due to their poor aerodynamic performance at low speeds. Future space plane may fly at high angle of attack even at transonic and supersonic speeds in the reentry phase.

When an aircraft with delta wing flying at high angle of attack in low speeds, there appear two large counter-rotating leading edge vortices. However, when an aircraft with delta wing flies at much higher speeds, the

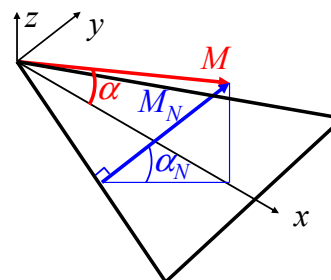


Figure 1. Definition of α_N and M_N

¹ Assistant professor, Department of Space Transportation Engineering, 3-1-1 Yoshinodai, AIAA Member.

² Graduate student, Department of Aeronautics and Astronautics, 3-1-1 Yoshinodai, currently Mitsubishi Heavy Industries, LTD., Non-member.

³ Graduate student, Department of Science and Engineering, Ishizaka, Non-member.

⁴ Professor, Department of Space Transportation Engineering, 3-1-1 Yoshinodai, AIAA Fellow.

flow becomes complicated because there appear shock waves which interact with vortices.

The earliest attempt to understand supersonic flows around delta wings at various flow conditions for various wing geometries appeared in the work of Stanbrook and Squire¹. By examining all the experimental data available, Stanbrook and Squire proposed a classification of the flow patterns based on the component of angle of attack normal to the leading edge α_N and the component of Mach number normal to the leading edge M_N (Fig. 1, eqs. (1) and (2)). They classified the flows into two types; attached flow and separated flow at the leading edge. The boundary line between these two types exists near $M_N = 1.0$, and has come to be known as the Stanbrook-Squire boundary (Fig. 2). Miller and Wood² experimentally studied flows over delta wings with different leading edge sweep angles using oil flow, tufts, and vapor screen methods. They classified the flows into six patterns according to α_N and M_N , namely (I) Classical vortex, (II) Vortex with shock, (III) Separation bubble with shock, (IV) Shock-induced separation, (V) Shock with no separation and (VI) Separation bubble with no shock (Fig. 2). Szodruch and Peake³, Seshadri and Narayan⁴, and Brodetsky⁵ also suggested similar classifications according to α_N and M_N .

$$M_N = M_\infty \cos(1 + \sin^2 \alpha \tan^2 \Lambda)^{1/2} \quad (1)$$

$$\alpha_N = \tan^{-1}(\tan \alpha / \cos \Lambda) \quad (2)$$

Recently, Imai, Fujii and Oyama⁶ computed flow fields of a 65-degree sweep delta wing at high angles of attack. While they discussed the flow mechanism behind the flow type classification, they did not mention relation between the flow types and aerodynamic characteristics of a delta wing at high angle of attack, which are very important for aircraft design.

Therefore, objective of the present study is to investigate aerodynamic characteristics of a delta wing and to reveal relation between flow type and the aerodynamic characteristics. To achieve this goal, flow fields over a delta wing at various angles of attack and various free-stream Mach numbers from subsonic to supersonic flow are computationally simulated and the aerodynamic characteristics and flow type of a delta wing are discussed.

II. Approaches

A. Numerical Methods

The governing equations are the three-dimensional compressible (Favre-averaged) Navier-Stokes equations. Length, density and velocities are normalized by the length of root chord, the density and the speed of sound of the free-stream, respectively. Numerical fluxes for the convective terms are evaluated by the AUSM-DV⁷ scheme extended to high-order space accuracy by the 3rd order upwind biased MUSCL interpolation⁸ based on the primitive variables. The viscous terms are evaluated by the 2nd order central differencing. The LU-ADI factorized implicit algorithm⁹ is used for the time integration. The flow fields are considered to be fully turbulent, and Baldwin-Lomax's algebraic turbulence model¹⁰ with Degani-Schiff's modification is applied.

B. Model Geometry and Grid

The model geometry is shown in Fig. 3. The delta wing analyzed here has leading-edge sweep angle of 65 degrees. The leading edge is sharp and lee-surface is flat to reduce the effect of leading-edge shape on flow fields. Wing thickness ratio is 0.02 based on each chord length.

The flow fields are assumed to be symmetric on center line of the wing. Therefore, the computational domain covers only half of the wing. The computational grid (Fig. 4) is H-O topology with grid size of 2.16 million (153(chordwise) x 143(spanwise) x 99(normal)).

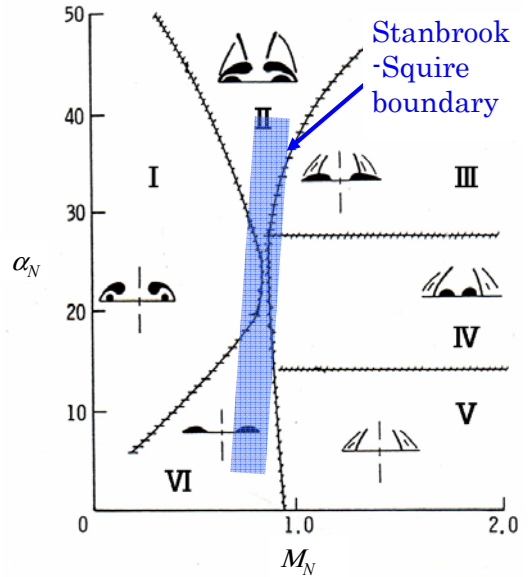


Figure 2. Flow fields classification chart by Miller and Wood².

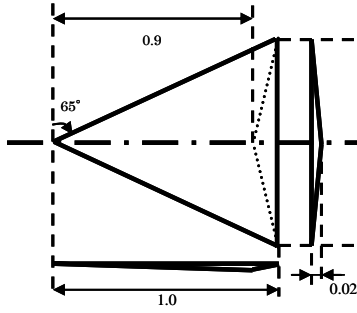


Figure 3. Model geometry.

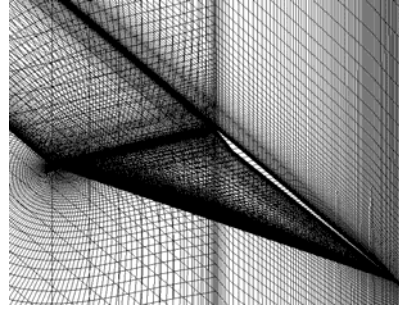


Figure 4. Computational grid.

C. Flow Conditions

The flow conditions are chosen to cover the classification chart of Miller and Wood². Free-stream Mach number covers from 0.4 to 3.2 and angles of attack covers from 4 to 24 degrees (increment 4 degrees). The selected Reynolds number based on the wing root-chord length is 1.3×10^6 according to the experiment of Miller and Wood.

D. Data Processing

Local time stepping method is used in the beginning of computations for shorter turn around time. After the solutions converge to certain extent, physical time stepping method is employed in the computations. All of the flow fields and the aerodynamic coefficients in the following discussions are based on the time-averaged physical variables.

III. Results and Discussions

A. Validation of the Present Computational Approach

To validate present computational approach, obtained data are compared with the experimental data of Miller and Wood¹¹. Figure 5 compares computed and measured spanwise distributions of static pressure on the upper surface at 95% chord position at some flow conditions. This figure shows the present approach is adequate to qualitative discussion of the aerodynamic characteristics of the present delta wing.

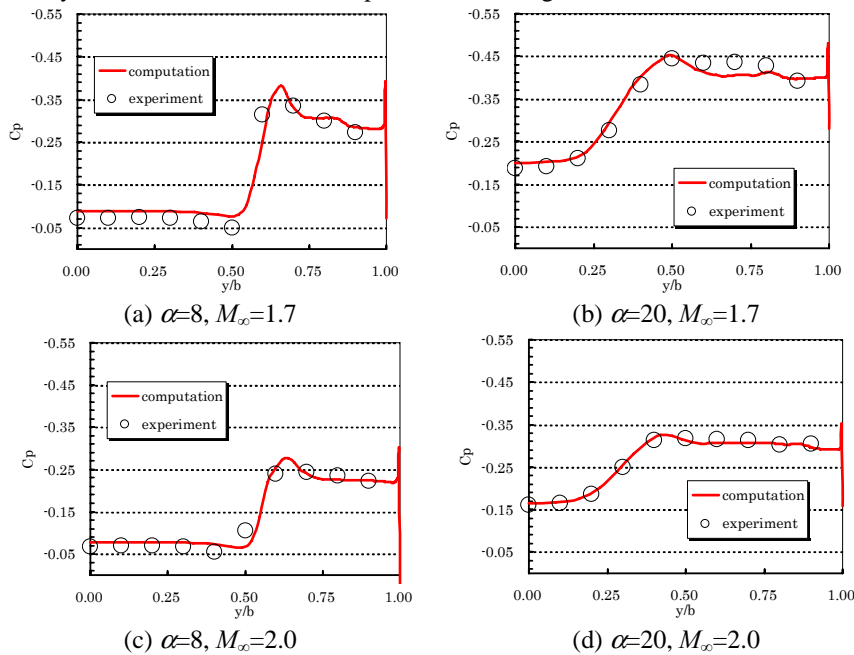


Figure 5. Comparison of computed and measured spanwise static pressure distributions.

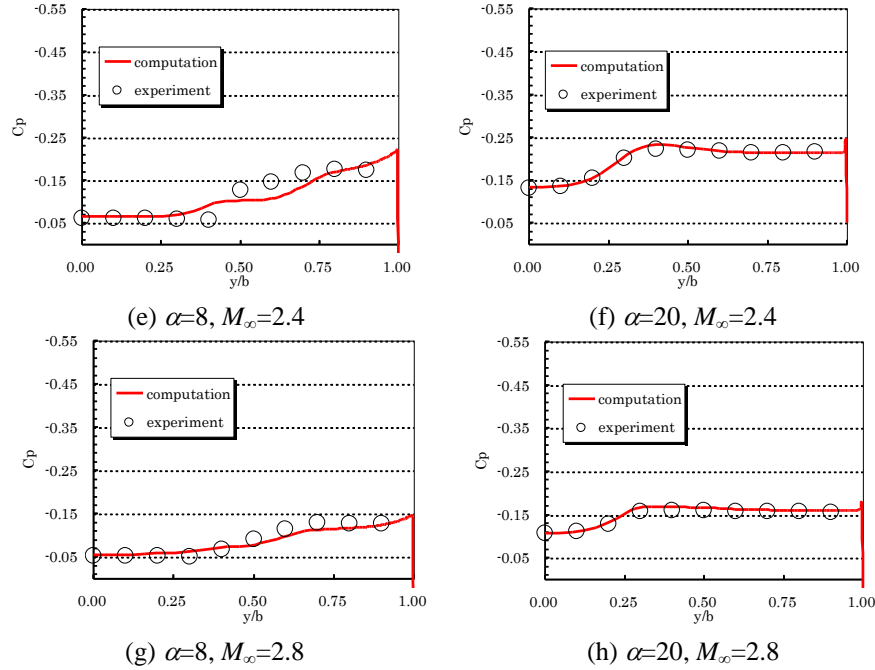


Figure 5. Comparison of computed and measured spanwise static pressure distributions (cont.).

B. Flow Field Classification

Computational results at the given flow conditions are classified according to the vortex structure in the crossflow plane at 30% chordwise location. The results are compared with classification chart of Miller and Wood in Fig. 6. Here, flows with or without any shock waves are denoted by open or closed symbols, respectively. The circular symbols denote that primary and secondary vortices appear in the flow fields. The square symbols denote that the flows are dominated by separation bubbles. This figure shows that the present results are classified into almost the same types as those in the experimental results of Miller and Wood. Note that the classification changes according to chordwise location as vortex breakdown occurs in some cases.

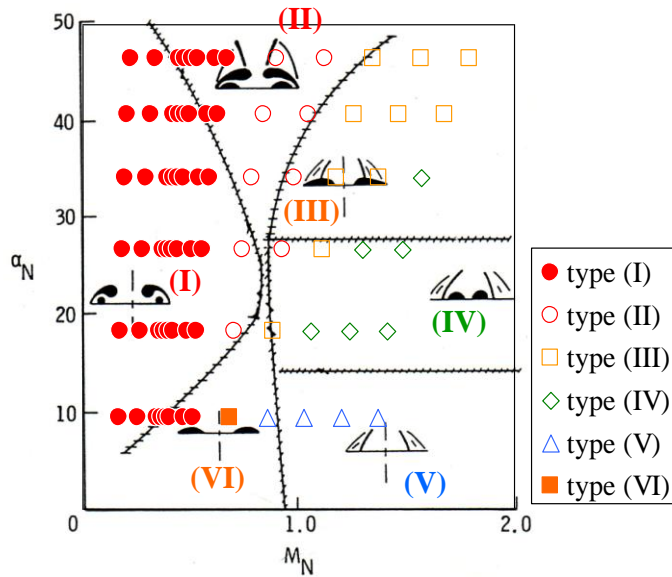


Figure 6. Flow classification of the present calculation result compared with the classification chart of Miller and Wood.

C. Aerodynamic characteristics

1. Normal force characteristics

Contour maps of normal force coefficient compared with the classification of Miller and Wood are presented in Fig. 7. A singular curve is observed in the contour maps near M_N of 0.5, i.e., M_∞ of 1.0, which does not correspond to any boundary of the classification of Miller and Wood or the present computational result (see Fig. 6). Also, any remarkable change in the contour maps is not observed on the boundaries of the classification of Miller and Wood. This means flow type change does not affect normal force of the delta wing very much. Instead, free stream Mach number affects the normal force characteristics.

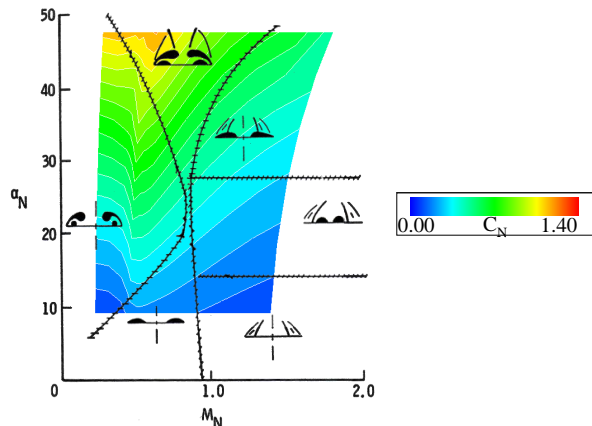
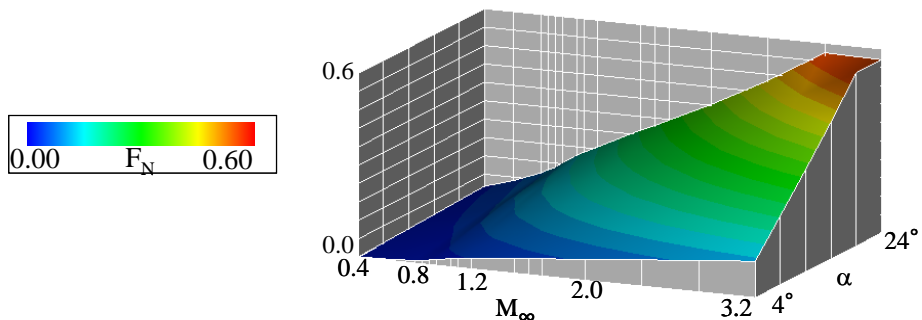
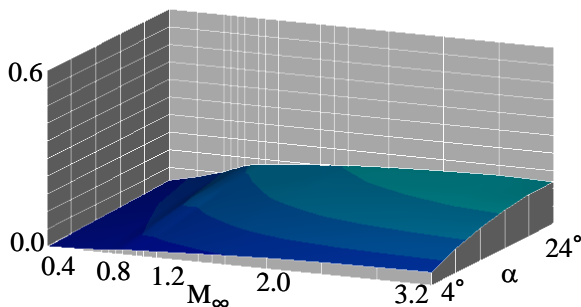


Figure 7. Normal force coefficient characteristics compared with the flow classification².

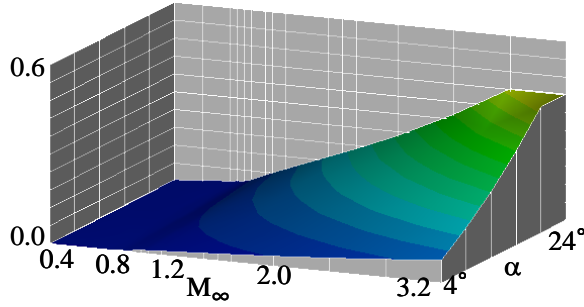
Figure 8 presents distributions of F_N (normal force acting on the upper and lower wing surfaces), normal force acting on the upper wing surface, and normal force acting on the lower wing surface. The normal force acting on the upper wing surface gradually increases as the free stream Mach number increases in the subsonic region while it is almost constant in the supersonic flow region. The normal force acting on the lower wing surface is almost zero in the subsonic region while it linearly increases in the supersonic region. These trend changes contribute to the nonlinear change in C_N and F_N in the transonic region.



(a) F_N (normal force acting on the upper and lower wing surfaces)



(b) Normal force acting on the upper wing surface



(c) Normal force acting on the lower wing surface

Fig. 8 Normal force distribution at the given flow conditions.

Figures 9 and 10 are upper surface pressure distributions in subsonic and transonic flow conditions at angle of attack of 8 and 20 degrees, respectively. These figures indicate that at both angles of attack, negative normal force on the upper surface increase as free-stream Mach number increases in subsonic and transonic flow conditions due to stronger primary vortex.

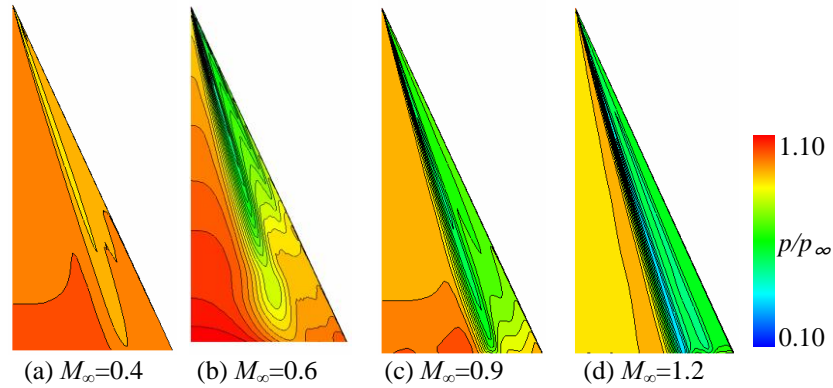


Figure 9. Upper surface pressure distributions in subsonic/transonic regions at angle of attack of eight degrees.

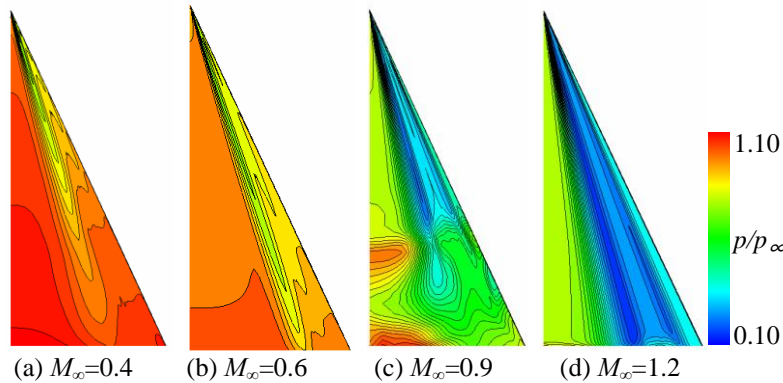


Figure 10. Upper surface pressure distributions in subsonic/transonic regions at angle of attack of twenty degrees.

Upper surface pressure distributions in supersonic flow conditions at angle of attack of 8 and 20 degrees are shown in Figs. 11 and 12. At both angles of attack, the spanwise surface pressure distribution is constant from the wing apex to the wing trailing edge. This figure also shows that the upper surface pressure distribution and negative normal force on the upper surface do not change very much in high supersonic flow region ($M_\infty > 2.0$). The reasons are 1) flow attachment for angle of attack of 8 degree cases, 2) very small (almost zero) surface pressure for angle of attack of 20 degree cases.

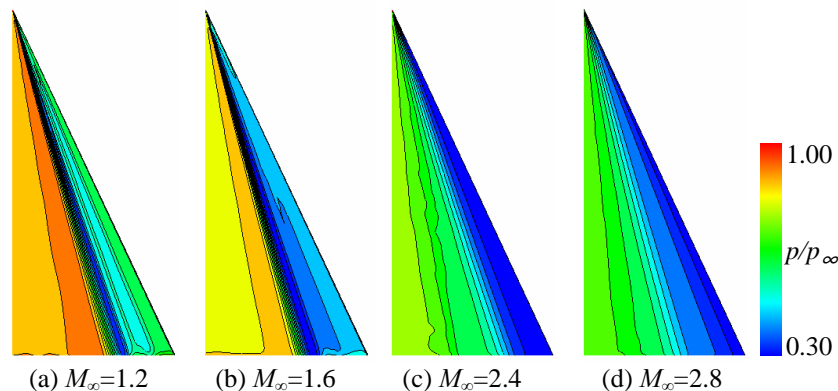


Figure 11. Upper surface pressure distributions in supersonic region at angle of attack of eight degrees.

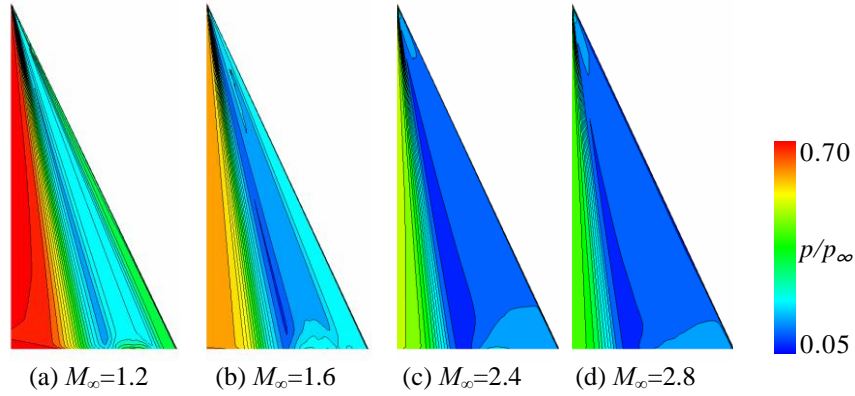


Figure 12. Upper surface pressure distributions in supersonic region at angle of attack of twenty degrees.

Figures 13 and 14 are pressure distributions on the computational symmetry plane at angle of attack of eight and twenty degrees, respectively. In subsonic flow, pressure increase on the lower surface is small. On the other hand, in supersonic flow, pressure on the lower surface increases as the free-stream Mach number increases due to the strong shock wave from the leading edge. This mainly contributes to normal force increase in the supersonic region. Corresponding surface pressure distributions are presented in Figs. 15 and 16. In subsonic flow, the surface pressure decreases toward the trailing edge while the spanwise pressure distribution is constant except for the vicinity of the trailing edge.

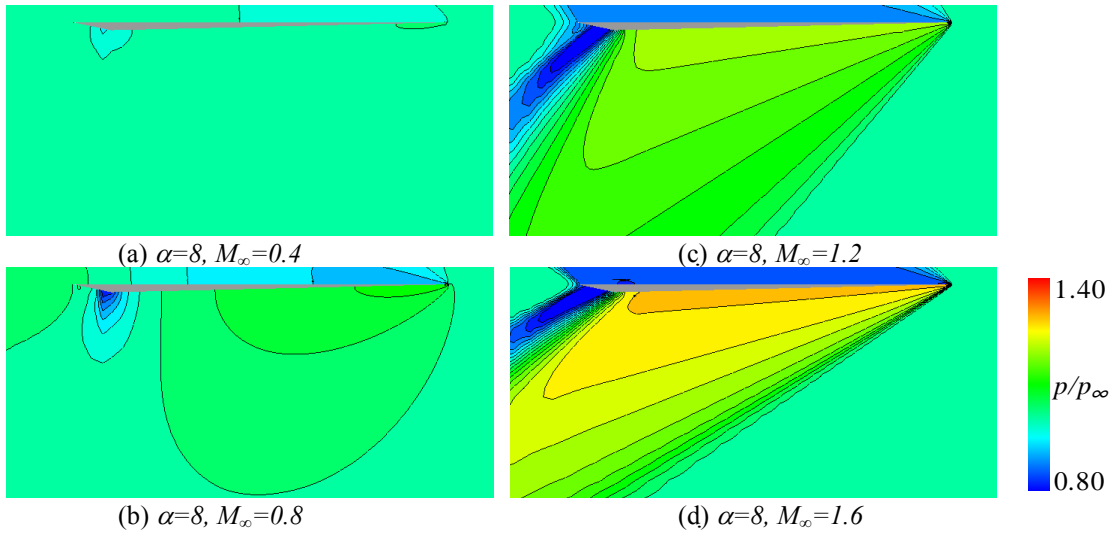


Figure 13. Pressure distributions on the symmetry plane at angle of attack of eight degrees.

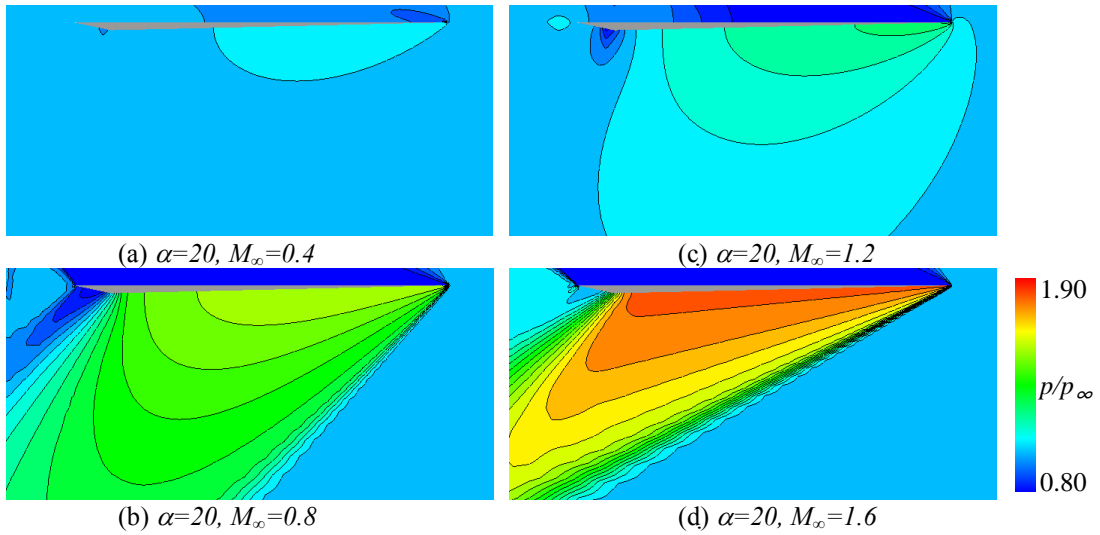


Figure 14. Pressure distributions on the symmetry plane at angle of attack of twenty degrees.

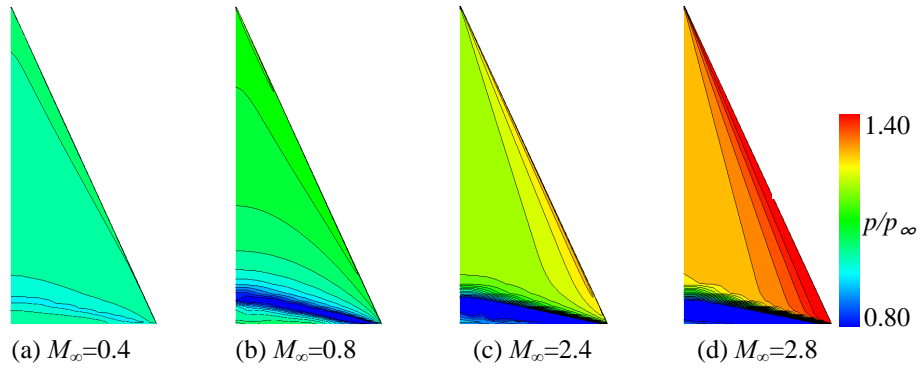


Figure 15. Lower surface pressure distributions at angle of attack of eight degrees.

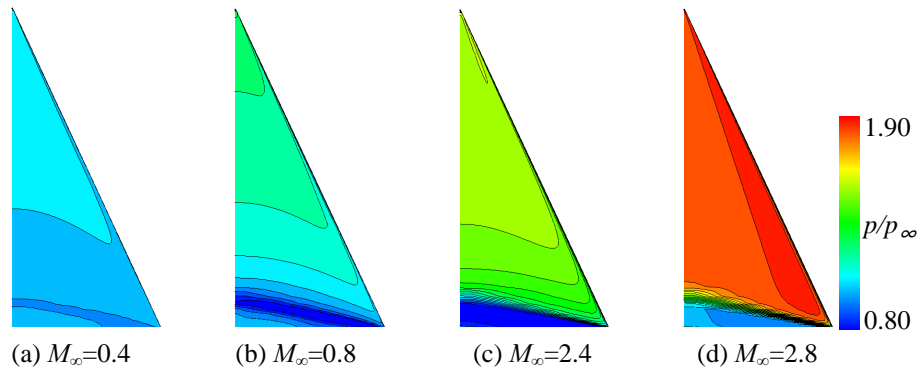


Figure 16. Lower surface pressure distributions at angle of attack of twenty degrees.

2. Pitching moment characteristics

Figure 17 is contour maps of pitching moment coefficient and pitching moment about the apex of the wing compared with the classification of Miller and Wood. As observed in the normal force characteristics, there is no significant change in pitching moment characteristics on the flow type boundaries.

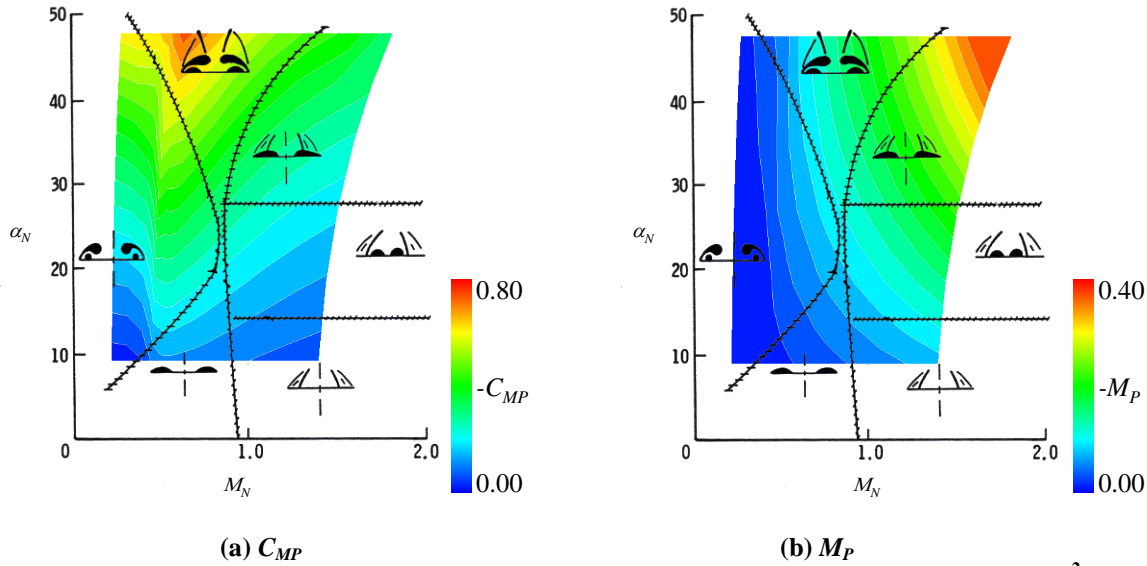


Figure 17. Pitching moment characteristics compared with the flow classification².

Free-stream Mach number effect on chordwise location of the center of pressure is presented in Fig. 18. The center of pressure moves toward trailing edge in transonic flow region. This is because effect of leading edge separation bubble is dominant on the upper surface pressure distribution in supersonic region (compare Figs 11 and 13, for example). This plot indicates that in addition to non-linear change in normal force in transonic region, change in chordwise location of the center of pressure contributes to the singular change in pitching moment contours in the transonic region.

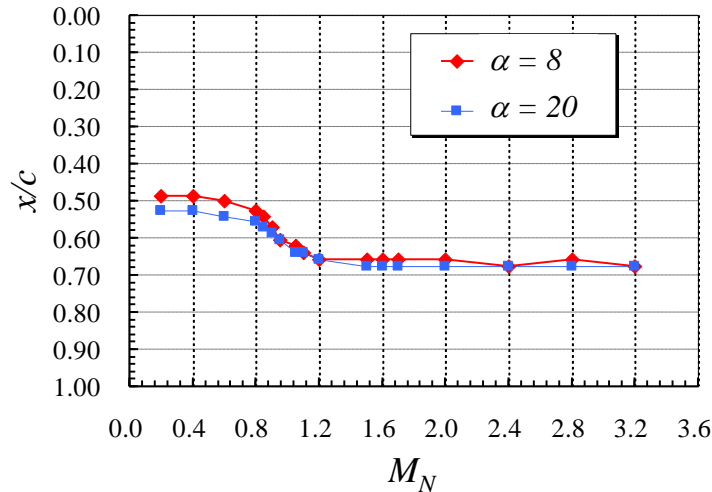


Figure 18. Free-stream Mach number effect on chordwise location of center of pressure.

3. Rolling moment characteristics

Figure 19 is contour maps of rolling moment coefficient and rolling moment about the root of the wing compared with the classification of Miller and Wood. As observed in the normal force and pitching moment characteristics, a singular curve is observed in the contour maps at M_N of 0.5.

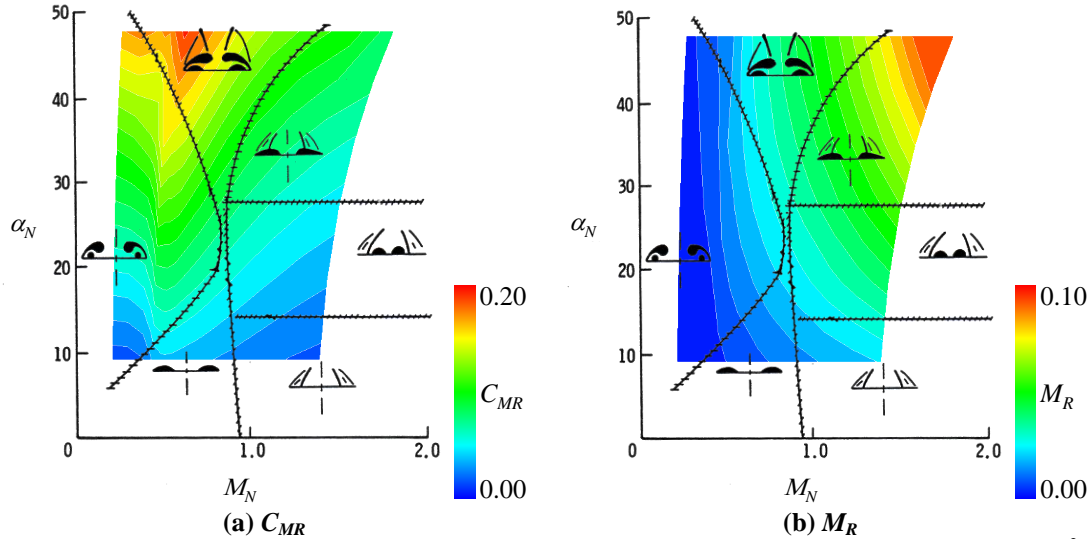


Figure 19. Rolling moment characteristics compared with the flow classification².

IV. Summary

In the present study, subsonic to supersonic flows over a delta wing at high angles of attack and corresponding aerodynamic characteristics of the delta wing have been computationally investigated. The results show that the flow type change does not significantly change the aerodynamic characteristics of the delta wing such as normal force, pitching and rolling moments. In stead, these aerodynamic force and moments significantly changes in the transonic region, which comes from trend change of both upper and lower surface pressure distributions in the transonic region.

References

- ¹Stanbrook, A., and Squire, L. C., "Possible Types of Flow at Swept Leading Edges," *Aeronautical Quarterly*, Vol.15, No. 2, pp. 72-82, 1964.
- ²Miller, D. S., and Wood, R. M., "Leeside Flows over Delta Wings at Supersonic Speeds," *Journal of Aircraft*, Vol. 21, No. 9, pp. 680-686, 1984.
- ³Szodrich, J. G., and Peake, D. J., "Leeward Flow over Delta Wings at Supersonic Speeds," NASA-TM, No. 81187, 1980.
- ⁴Seshadri, S. N., and Narayan, K. Y., "Possible Types of Flow on Lee-Surface of Delta Wings at Supersonic Speeds," *Aeronautical Journal*, Vol.92, No.915, pp. 185-199, 1988.
- ⁵Brodetsky, M. D., Krause, E., Nikiforov, S. B., Pavlov, A. A., Kharitonov, A. M., and Shevchenko, A. M., "Evolution of Vortex Structures on the Leeward Side of a Delta Wing," *Journal of Applied Mechanics and Technical Physics*, Vol. 42, No. 2, pp. 242-254, 2001
- ⁶Imai, G., Fujii, K., and Oyama, A., "Computational Analyses of Supersonic Flows over a Delta Wing at High Angles of Attack," 25th International Congress of the Aeronautical Sciences, 2006
- ⁷Wada, Y., and Liou, M. S., "A Flux Splitting Scheme with High-Resolution and Robustness for Discontinuities," AIAA paper 1994-0083, 1994
- ⁸Van Leer, B., "Toward the Ultimate Conservative Difference Scheme. 4," *Journal of Computational Physics*, Vol. 23, pp. 276-299, 1977.
- ⁹Fujii, K., and Obayashi, S., "Practical Applications of New LU-ADI Scheme for the Three-Dimensional Navier-Stokes Computation of Transonic Viscous Flows," AIAA paper 1986-513, 1986.
- ¹⁰Baldwin, B., and Lomax, H., "Thin Layer Approximation and Algebraic Model for Separated Turbulent Flows," AIAA paper 1978-257, 1978.
- ¹¹Miller, D. S., and Wood, R. M., "Lee-side Flow over Delta Wings at Supersonic Speeds," NASA-TP 2430, 1985.